Inorg. Chem. **1994**, *33*, 3481–3486 **3481**

Structural Study of Triangulated Heterometallic Metal Clusters with a Molecular Fragment (μ-PR_2)Re_2M in $Re_2(\mu\text{-}PR_2)(CO)_8[\mu\text{-}M(CO)_2PPh_3]$ (M(I) = Rh, Ir; R = Ph, Cy) and in $Re_2Rh(\mu\text{-}CO)_2(\mu\text{-}PR_2)(CO)_6(PPh_3)_2$ with a Rhenium–Rhodium Double Bond

H.-J. Haupt,[*] U. Flörke, and H.-G. Beckers

Department of Inorganic and Analytical Chemistry, University-GH Paderborn, 33098 Paderborn, FRG

Received September 29, 1993[•]

In tetrahydrofuran solution redox condensation reactions between the salts $NEt_4[Re_2(\mu\text{-}PR_2)(CO)_8]$ (R=Ph, Cy) and $ClM(CO)(PPh_3)_2$ (M = Rh, Ir) in the presence of the chloride scavenger $TlPF_6$ and CO(g) at 20 °C in 3 h gave four red compounds of the type $Re_2(\mu\text{-}PR_2)(CO)_8[M(CO)_2PPh_3]$ (M = Rh, R = Ph (**1**) and Cy (**2**); M = Ir, R = Ph (**3**), and Cy (**4**)) which were separated. The remaining two red title compounds $ReRh(\mu\text{-}CO)_2(\mu\text{-}PR_2)(CO)_2(PPh_3)_2[Re(CO)_4]$ (R = Ph (**5**), Cy (**6**)) were obtained from the reaction of $[Rh(COD)(PPh_3)_2]BF_4$ and the aforementioned dirhenium salts in thf solution under reflux conditions within 20 h. **1**–**4** were characterized by ^{31}P NMR, ν(CO) IR, and UV/vis spectroscopic data. The molecular structures of the saturated triangular cluster complexes **1** and **4** and that of unifold unsaturated **6** were identified by single-crystal X-ray data. Compounds **1**, **4**, and **6** crystallize in the monoclinic space groups $P2_1/n$ (Z = 4), $P2_1/c$ (Z = 8), and $P2_1/n$ (Z = 4). For **1**, a = 12.138(2) Å, b = 23.376(4) Å, c = 14.019(3) Å, and β = 90.65(2)°; for **4**, a = 12.694(3) Å, b = 20.700(3) Å, c = 32.769(6) Å, and β = 101.06(1)°; and for **6**, a = 12.757(3) Å, b = 32.106(7) Å, c = 13.999(3) Å, and β = 94.04(2)°, respectively. The (μ-P)Re_2M core in **1** and **4** is planar. These bridged Re atoms have octahedrally distorted ligand environments, while the M atoms are coordinated pseudotrigonal bipyramidally by two axial CO groups, an equatorial PPh_3, and two equatorial Re atoms. The values of the σ(Re–Re) and average σ(Re–M) bond lengths are 3.169(1) and 2.988(1) Å in **1** and 3.133(1) and 2.962(1) Å in **4**. In spite of lacking steric strain at both heterometallic Re–M edges in each of the considered compounds, there are unusual structural differences. Particularly the σ bond lengths along the Re–M edges and the exocyclic bond angles Re–M–P differ by 0.091(1) Å and 20.2(1)° in **1** or by 0.100(1) Å and 20.0(3)° in **4**. These differences were discussed. The central molecular fragment of **6** contains a Re_2Rh ring of which one Re–Rh edge is bridged by two carbonyls and the other by a dicyclohexylphosphido group and the Re–Re edge remains unbridged. At the Rh atom the ligand atoms (2C, 2P) are attached in pseudotetrahedral arrangement which is completed by two Re atoms to a [4 + 2] coordination pattern. The CO bond vector of each bridging carbonyl is inclined toward the Rh atom. The σ(Re–Rh) and the π(Re–Rh) bond lengths are 2.883(1) and 2.681(1) Å, respectively. The unsupported Re–Re bond contact length is 3.255(1) Å.

Introduction

This study continues our recent work on reactions between ditransition metal carbonyl anions or derivatives and ligated metal cations which, via a redox condensation process, yielded triangulated mixed-metal clusters of the types $M'_2(\mu\text{-}PR_2)(CO)_8(MPPh_3)$ (M′ = Mn, Re; M = Ag, Au) and $ReMo(\mu\text{-}PPh_2)(CO)_6(\eta\text{-}C_5H_5)(MPPh_3)$ (M = Cu, Ag, Au).[1-3] In terms of the isolobal concept,[4] the generation of such cluster types is based on an isolobal exchange of a proton in related hydrido/phosphido-bridged precursor complexes against a cation MPh_3^+. In the case of the title compounds **1**–**4** which are also obtained by such a redox process, the mentioned concepts demonstrate formally the successful possibility of combining methylene-like cations $M(CO)_2PPh_3^+$ (M = Rh, Ir) and cyclopropanyl-like anions $[Re_2(\mu\text{-}PR_2)(CO)_8]^-$ to form bicyclo[1.1.0]butane-like clusters.[4,5] The single-crystal X-ray analyses of **1** and **4** showed for the M atoms a cn (coordination number) of 5 in a pseudo-trigonal bipyramidal coordination sphere which is in contrast to the usually preferred square planar ligand arrangement.[6] Resulting changes of structural parameters are discussed as well as the molecular structure of **6** with the first π(Re–Rh) bond determined. Common for all these cluster complexes **1**–**6** are nontypical cn's for Rh and Ir atoms.

Experimental Section

The reactions were performed in deoxygenated solvents dried by standard methods under an argon atmosphere.

Materials. Both substances of the type $M(CO)(PPh_3)_2Cl$ (M = Rh, Ir) and $Rh(COD)(PPh_3)BPh_4$ were prepared according to the literature method.[7,8] $Re_2(CO)_{10}$, $TlPF_6$, and HPR_2 (R = phenyl, cyclohexyl) were purchased from Strem Chemicals.

Preparation of the Compounds $Re_2[\mu\text{-}PR_2)(\mu\text{-}M(CO)_2PPh_3](CO)_8$ (M = Rh, R = Ph (1), Cy (2); M = Ir, R = Ph (3), Cy (4)). In a 100-mL round-bottom flask equipped with a gas inlet, each 0.13 mmol sample of $M(CO)(PPh_3)_2Cl$ (Rh, 85 mg; Ir, 102 mg)[7] and that of the chloride acceptor $TlPF_6$ (50 mg; 0.14 mmol) were stirred in 20 mL of tetrahydrofuran at 20 °C for 1 h. The equivalent amount of the salt $NEt_4[Re_2(\mu\text{-}PR_2)(CO)_8]$ (R = Ph (118 mg), Cy (120 mg); 0.13 mmol)[1,9] was added, and then in the reaction time of 2 h a continuous stream of CO(g) was introduced into the solution which changed the color from yellow to red. Colorless thallium(I) chloride was precipitated. To separate the products, the precipitate of TlCl was removed by centrifugation and the solution evaporated to dryness. The remaining solid was suspended in dichloromethane for removal of unsoluble salts $NEt_4[PF_6]$ and $Rh(CO)_2$-

---

[•] Abstract published in *Advance ACS Abstracts*, July 1, 1994.

(1) Haupt, H.-J.; Heinekamp, C.; Flörke, U. *Inorg. Chem.* **1990**, *29*, 2955.

(2) (a) Haupt, H.-J.; Heinekamp, C.; Flörke, U.; Jüptner, U. *Z. Anorg. Allg. Chem.* **1992**, *608*, 100. (b) Heinekamp, C. Dissertation, University of Paderborn, 1990.

(3) Haupt, H.-J.; Flörke, U.; Disse, G.; Heinekamp, C. *Chem. Ber.* **1991**, *124*, 2191.

(4) Hoffmann, R. *Angew. Chem.* **1982**, *94*, 725.

(5) Stone, F. G. A. *Angew. Chem.* **1984**, *96*, 85.

(6) Hughes, R. P. In *Comprehensive Organometallic Chemistry*; Wilkinson, G., Stone, F. G. A., Abel, E., Eds.; Pergamon Press: Elmsford, NY, 1982; Chapter 35.

(7) Shapley, J. R.; Schrock, R. R.; Osborn, J. A. *J. Am. Chem. Soc.* **1969**, *91*, 2816.

(8) Schrock, R. R.; Osborn, J. A. *J. Am. Chem. Soc.* **1971**, *93*, 2397.

(9) Merla, A.; Flörke, U.; Haupt, H.-J. *Z. Anorg. Allg. Chem.* **1994**, 620, 999.

0020-1669/94/1333-3481$04.50/0

Table 1. Crystallographic Data for **1**, **4**, and **6**[a]

	1	**4**	**6**
formula	$C_{40}H_{25}O_{10}P_2Re_2Rh$	$C_{40}H_{37}IrO_{10}P_2Re_2$	$C_{56}H_{52}O_8P_3Re_2Rh\cdot CHCl_3$
mol wt	1202.9	1304.3	1540.6
cryst size, mm	0.10 × 0.13 × 0.40	0.08 × 0.11 × 0.43	0.19 × 0.28 × 0.56
space group (No.)	$P2_1/n$ (14)	$P2_1/c$ (14)	$P2_1/n$ (14)
a, Å	12.138(2)	12.694(3)	12.757(3)
b, Å	23.376(4)	20.700(3)	32.106(7)
c, Å	14.019(3)	32.769(6)	13.999(3)
β, deg	90.65(2)	101.06(2)	94.04(2)
V, Å^3	3977.5(12)	8450.6(30)	5719.4(25)
Z	4	8	4
D_{calc}, g cm^{-3}	2.009	2.050	1.789
$F(000)$	2280	4912	3000
μ, mm^{-1}	6.69	9.05	4.84
transm coeff	0.72/0.53	0.79/0.56	0.88/0.52
R, R_w	0.042, 0.031	0.070, 0.053	0.046, 0.043

[a] For all the structures, Mo Kα radiation was used and $T = 298$ K. $w = 1/\sigma^2(F) + 0.0001F^2$. $R = \sum(|F_o| - |F_c|)/\sum|F_o|$; $R_w = \{\sum w(|F_o| - |F_c|)^2/\sum w|F_o|^2\}^{1/2}$.

$(PPh_3)_2[PF_6]$ by filtration before the desired component of each reaction system, finally, was obtained by use of a preparative HPLC separation procedure (Fa. Merck, LiChrograph: gradient pump and system L-6200, UV detector with λ = 286 nm, flow rate of 3 mL/min). By using different CH_2Cl_2/*n*-hexane solvent mixtures (**1**, 1/1; **2**, 1/2; **3**, 2/3; **4**, 1/3), small amounts of $Re_2(\mu\text{-}H)(\mu\text{-}PR_2)(CO)_8$[1] formed by the reprotonation of anions $[Re_2(\mu\text{-}PR_2)(CO)_8]^-$ could be separated from products **1**–**4** which had in each case a longer retention time (>12 min). The components in the fractions obtained were identified by accompanying ^{31}P NMR measurements. Each solvent mixture was then vacuum-stripped to leave a red solid which was crystallized by a vapor diffusion equilization method (CH_2Cl_2/*n*-pentane). Yield: **1**, 105 mg (60%); **2**, 131 mg (75%); **3**, 60 mg (32%); **4**, 73 mg (38%).

$Re_2Rh(\mu\text{-}CO)_2(\mu\text{-}PR_2)(CO)_6(PPh_3)_2$ (5, R = Ph; 6, R = Cy). A 0.13-mmol sample of $NEt_4[Re_2(\mu\text{-}PR_2)(CO)_8]$ (R = Ph, 118 mg; R = Cy, 120 mg) and 137 mg (0.13 mmol) of $[RhCOD(PPh_3)_2]BPh_4$[8] in 15 mL of thf solution were heated under reflux 20 h. The color of the solution changed from yellow to red. To separate the desired compounds, the solution was vacuum-stripped to leave a red solid; this residue was suspended in dichloromethane and filtered to remove saltlike compounds. The filtrate was evaporated to dryness, and finally, **5** was obtained by use of the TLC and **6** by that of the HPLC separation procedure. The components of single fractions were identified by ^{31}P NMR measurements. The first-named separation method (PSC plate, silica 60) with CH_2Cl_2/*n*-hexane (1/1) as eluant gave the following products from the corresponding number of fractions, listed in order of decreasing R_f values: colorless $Re_2(\mu\text{-}PPh_2)(\mu\text{-}H)(CO)_8$/$Re_2(\mu\text{-}H)(\mu\text{-}PPh_2)(CO)_7(PPh_3)$,[1,10] red **5** (39 mg; 21%), and a red compound unidentified with $\delta(^{31}P)$ NMR data [184.8 (dd, J values of 137.3 and 13.4 Hz), 30.1 (ddd, 221.4, 10.9, 6.1 Hz), 18.3 (d, 10.9 Hz), 15.0 (d, 8.5 Hz)]. The HPLC procedure with CH_2Cl_2/*n*-hexane (1/2) led to the subsequent products from an equivalent number of fractions, listed in order of decreasing retention time values: PPh_3, $Re_2(\mu\text{-}H)(\mu\text{-}PCy_2)(CO)_8$, and red **6** (24 mg; 13%). Red crystals of **5** and **6** could be obtained by application of the vapor diffusion method (CH_2Cl_2/*n*-hexane).

Analytical and Spectral Data. The spectral data obtained were recorded with the following spectroscopic equipment: ^1H and ^{31}P NMR, Bruker AMX 300 ($CDCl_3$ solution, 25 °C; TMS and H_3PO_4 (85%) as standards); Nicolet FT-IR 510 P/PCIR for compounds **5** and **6**, and Perkin-Elmer 1330 for **1**–**4** (CH_2Cl_2 solution), and Perkin-Elmer Lambda 15, UV/vis for **2** and **6** (CH_2Cl_2 solution).

Anal. Calc for **1**: C, 39.9; H, 2.1. Found: C, 40.42; H, 2.39. Calc for **2**: C, 39.5; H, 3.1. Found: C, 39.54; H, 3.08. Calc for **3**: C, 37.2; H, 1.9. Found: C, 37.46; H, 1.93. Calc for **4**: C, 36.8; H, 2.8. Found: C, 37.02; H, 2.68. Calc for **5**: C, 47.7; H, 2.8. Found: C, 47.79; H, 3.01. Calc for **6**: C, 47.3; H, 3.7. Found: C, 46.92; H, 3.62.

$\delta(^{31}P)$ NMR: **1**, 137.4 (d, μ-P, $^3J(PP)$ 7.3 Hz), 39.2 (dd, PPh_3, $^1J(PRh)$ 155.5 Hz, $^3J(PP)$ 7.3Hz); **2**, 163.8 (d, μ-P, $^3J(PP)$ 5.2 Hz), 39.8 (dd, PPh_3, $^1J(PRh)$ 148.6 Hz, $^3J(PP)$ 5.2 Hz); **3**, 164.5 (s, μ-P), 32.0 (s, PPh_3); **4**, 193.2 (s, μ-P), 31.3 (s, PPh_3); **5**, 205.1 (ddd, μ-P, $^1J(RhP)$ 151.9 Hz, $^2J(PP)$ 7.3 Hz, $^3J(PP)$ 10.3 Hz), 33.2 (dd, PPh_3, $^1J(PRh)$ 208.7 Hz, $^2J(PP)$ 6.6 Hz), 17.6 (d, PPh_3, $^3J(PP)$ 11.1 Hz); **6**, 259.5 (ddd, μ-P, $^1J(PRh)$ 138.5 Hz, $^2J(PP)$ 3.9 Hz, $^3J(PP)$ 11.8 Hz), 30.4 (dd, PPh_3, $^1J(PRh)$ 212.3 Hz, $^2J(PP)$ 3.5 Hz, 17.1 (d, PPh_3, $^3J(PP)$ 10.8 Hz).

Scheme 1

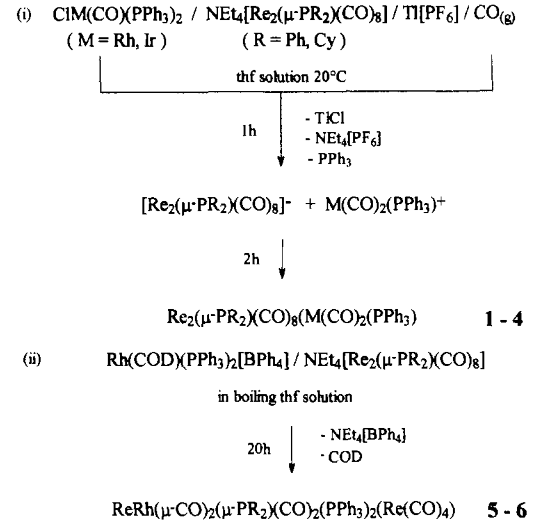

ν(CO) IR frequencies: **1**, 2045 m, 1998 vs, 1946 s, 1922 s; **2**, 2036 m, 1990 vs, 1944 s, 1917 s; **3**, 2044 m, 1994 vs, 1946 s, 1927 s; **4**, 2040 m, 1985 vs, 1944 s, 1925 s; **5**, 2068 s, 1995 vs, 1981 vs, 1966 vs, 1937 m, 1904 s, 1817 w; **6**, 2062 s, 1989 vs, 1962 vs, 1935 m, 1902 s, 1810 w.

UV/vis electron absorption transfer: λ_{max} 335 nm (ϵ 1630 m^2 mol^{-1}), 387 nm (ϵ 1038 m^2 mol^{-1}), and 482 nm (ϵ 1078 m^2 mol^{-1}; CT, σ–σ^*) in **2**; λ_{max} 279 nm (1485 m^2 mol^{-1}), 311 nm (ϵ 1741 m^2 mol^{-1}), 423 (sh) (ϵ 332 m^2 mol^{-1}), and 504 nm (ϵ 142 m^2 mol^{-1}; π–π^*) in **6**.

Structure Determination of 1. Lattice parameters were refined from 30 reflections with $15 \le 2\theta \le 39°$. Data were collected on a Siemens R3m/V diffractometer, ω–2θ scan, $3 \le 2\theta \le 55°$, 9890 intensities. Three standards recorded every 400 measurements showed only random deviations. Lp and empirical absorption corrections (ψ-scans) were performed; after merging ($R_{int} = 0.035$) 5477 unique observed intensities with $F > 4\sigma(F)$ were observed. The structure was solved by direct and Fourier methods. Full-matrix least-squares refinement was based on F and 436 parameters, with all but H-atoms refined anisotropically, phenyl groups treated as rigid bodies (C–C = 1.395 Å), and H-atoms fixed at idealized positions with common isotropic displacement parameters $U_{iso} = 0.08$ Å^2. Residuals in final ΔF map: −0.8 and 0.9 e/Å^3. Further information is given in Table 1. Scattering factors, structure solution, and refinement: SHELXTL-Plus.[11] Other programs: PARST,[12] MISSYM.[13]

Structure Determination of 4. Lattice parameters were refined from 47 reflections with $10 \le 2\theta \le 30°$. Data collection was as before with $3 \le 2\theta \le 50°$ and 15 613 intensities. Standards and corrections were as before; after merging ($R_{int} = 0.053$) there were 7203 unique observed intensities with $F > 4\sigma(F)$. Structure solution and refinement as before, with Re, Ir, and P refined anisotropically, 419 parameters, 2 independent

---

(10) Haupt, H.-J.; Balsaa, P.; Flörke, U. *Z. Anorg. Allg. Chem.* **1987**, *548*, 151.

(11) Sheldrick, G. M. SHELXTL-Plus. Siemens Analytical X-ray Instruments, Inc., Madison, WI, 1990.

(12) Nardelli, M. *Comput. Chem.* **1983**, *7*, 95.

(13) Le Page, Y. J. *Appl. Crystallogr.* **1987**, *20*, 264.

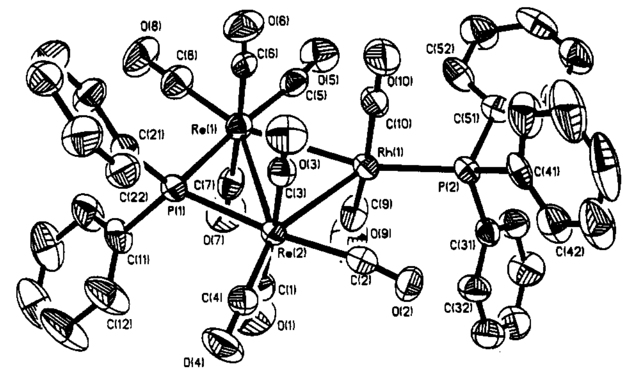

Figure 1. Molecular structure of **1**. Hydrogen atoms are omitted. The ORTEP plot shows 50% probability for the thermal ellipsoids.

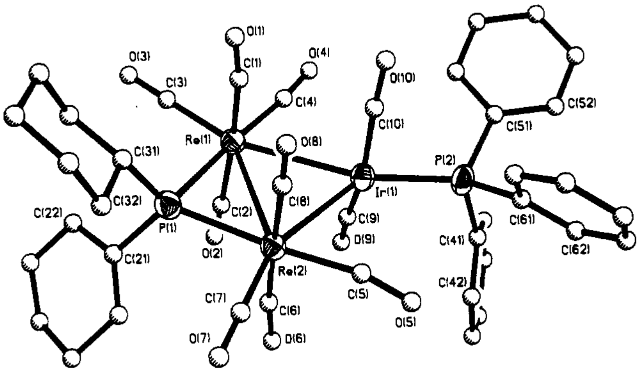

Figure 2. Molecular structure of **4**. Hydrogen atoms are omitted. The ORTEP plot shows 50% probability for the thermal ellipsoids.

molecules per asymmetric unit, and residuals in the final ΔF map of -1.3 and 1.1 e/Å^3 near the heavy atom positions.

Structure Determination of 6. Lattice parameters were refined from 33 reflections with $12 \leq 2\theta \leq 33°$. Data collection was as before, with $3 \leq 2\theta \leq 52°$ and 11 854 intensities. Standards and corrections were as before; after merging (R_{int} = 0.046) there were 7611 unique observed intensities with $F > 4\sigma(F)$. Structure solution and refinement were as for **1**, with 595 parameters and residuals in the final ΔF map of -0.9 and 0.8 e/Å^3.

Results and Discussion

Preparation. In thf solution the new members **1–4** in the family of mixed-metal triangular clusters[14,15] with one diorganophosphido bridge are synthesized by a redox condensation process between the anions of the salts $NEt_4[Re_2(\mu\text{-}PR_2)(CO)_8]$ (R = Ph, Cy) and cations generated in an equilibrium reaction from $ClM(CO)(PPh_3)_2$ (M = Rh, Ir)[7] with the chloride scavenger $TlPF_6$ in the presence of CO(g) at 20 °C in 2 h. The product formation is shown in Scheme 1i. Of the dirhenium anions studies, those containing the bridging dicyclohexylphosphido group are more electron-rich than those bridged by the diphenylphosphido group, as confirmed by cyclic voltammetry.[1,2] These electron-rich anions give a higher yield of product. The molecular structures of **1** and **4** were determined from single-crystal X-ray analysis (Figures 1 and 2). Compounds **2** and **3** were found isostructural on the basis of Guinier powder patterns to those of **1–4**. For further characterization ^{31}P NMR and IR measurements of the dissolved compounds **1–4** were recorded (see Experimental Section).

The remaining title compounds **5** and **6** were prepared by heating $[Rh(COD)(PPh_3)_2]BF_4$ and the salts $NEt_4[Re_2(\mu\text{-}PR_2)(CO)_8]$ in thf solution over 18–20 h. Other rhodium salts like $ClRh(CO)(PPh_3)_2$ and $ClRh(PPh_3)_3$ were also utilized, but they give lower yields. The structure of **6** (Figure 3) was established by single-crystal X-ray analysis; on the basis of ν(CO) IR and ^{31}P NMR data, **5** has the same molecular structure.

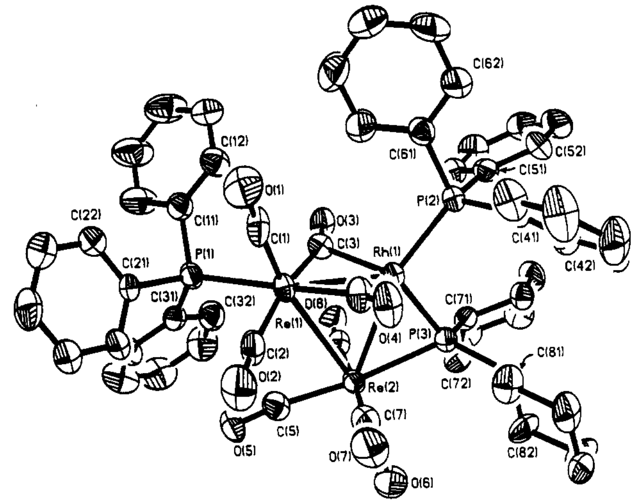

Figure 3. Molecular structure of **6**. Hydrogen atoms are omitted. The ORTEP plot shows 50% probability for the thermal ellipsoids.

As is known from similar compounds,[15,16] there might be an equilibrium between a carbonyl bridged and an unbridged species of **6** in solution. The best available solvent, $CDCl_3$, with a solubility of 21 μmol/2.5 mL was insufficient to get well-resolved ^{13}C NMR data to characterize such a fluxional process. Nevertheless, this process is indicated by temperature-dependent ^{31}P NMR measurements. On cooling of the sample from 293 to 231 K the 30.4 ppm (d, ^1J(PPh) 213 Hz) signal of the PPh_3 group attached to the Rh atom undergoes a shift to 31.4 ppm (d, ^1J(RhP) 213 Hz) and a new signal occurs at 29.1 ppm (d, ^1J(RhP) 122 Hz).

Structural Descriptions. Structural studies were undertaken for the cluster complexes **1**, **4**, and **6**, whose crystal data, positional parameters of selected atoms, and selected bond angles and bond lengths are presented in Tables 1–5. The molecular structures are shown in Figures 1–3.

Clusters 1 and 4. The molecules of both the diamagnetic compounds **1** and **4** (Figures 1 and 2) are of C_1 symmetry. Each central molecular fragment shows a four-membered planar $(\mu\text{-}P)Re_2M$ (M = Rh, Ir) ring. The maximum deviation of the P ring atoms from a best-fitted plane is 0.014 Å in **1** and 0.029 Å in **4**, respectively. Additionally, both rings have a transannular Re–Re bond to fulfill the demand of the noble gas rule. A view along the diorganophosphido-bridged Re–Re bond vector illustrates that the four corresponding pairs of terminal CO ligands are arranged in eclipsed positions. The same conformation is present in the related compounds $Re_2(\mu\text{-}H)(\mu\text{-}PPh_2)(CO)_7PPh_3$[10] and $[Re_2(\mu\text{-}PPh_2)(CO)_8(HgCl)]_2$[9] with three and four carbonyl pairs and indicates an absence of repulsive nonbonding forces between CO pairs. The coordination sphere of each Re atom is distorted octahedrally. Each of the remaining ring atoms M has two CO groups, one PPh_3 group, and both Re atoms as ligands, a coordination which is best described as pseudotrigonal bipyramidal with both carbonyls at the axial positions. Both acute endocyclic bond angles at the M atoms correlate with an opposite Re–Re bond of 3.169(1) Å in **1** and of average of 3.134(2) Å in **4**, whereas the obtuse exocyclic bond angles Re–M–P(2) show extraordinarily large differences of 20.2(1)° in **1** and an average of 20.0(3)° in **4**. The smaller Re(2)–M–P(2) bond angle is always situated at the shortened Re–M edge. The differences between the edges are 0.091(1) Å in **1** and an average of 0.100(2) Å in **4**, although at the same Re–M edges no steric strain is present which was proved by the analysis of intra- and intermolecular contacts. Besides that, these large differences are unusual for

---

(14) Iggo, A.; Mays, M. J.; Raitby, P. R.; Henrick, K. *J. Chem. Soc., Dalton Trans.* **1984**, 633.

(15) Adams, R. D.; Johnson, B. F. G.; Rodgers, A. In *The Chemistry of Metal Cluster Complexes*; Shriver, D. F., Kaesz, H. D., Adams, R. D., Eds.; VCH Publishers: New York, 1990; Chapters 3 and 7.

(16) Antonelli, D. M.; Cowie, M. *Organometallics* **1991**, *10*, 2550.

Table 2. $C_{40}H_{25}O_{10}P_2Re_2Rh$ (**1**): Selected Atomic Coordinates ($\times 10^4$) and Equivalent Isotropic Displacement Parameters (Å$^2 \times 10^3$)

	x	*y*	*z*	*U*(eq)[a]
Re(1)	6508(1)	928(1)	6549(1)	37(1)
Re(2)	6290(1)	506(1)	8686(1)	31(1)
Rh(1)	5165(1)	1552(1)	8034(1)	35(1)
P(1)	7262(2)	90(1)	7361(2)	38(1)
P(2)	4052(2)	2256(1)	8673(2)	39(1)
C(1)	7624(7)	944(4)	8993(6)	43(3)
O(1)	8424(5)	1181(3)	9175(5)	82(3)
C(2)	5408(6)	930(4)	9640(6)	36(3)
O(2)	4970(5)	1104(3)	10287(4)	50(2)
C(3)	4964(7)	44(4)	8329(6)	37(3)
O(3)	4213(5)	−224(3)	8130(5)	59(3)
C(4)	6746(7)	−35(4)	9622(6)	42(3)
O(4)	7053(5)	−356(3)	10198(5)	71(3)
C(5)	5810(7)	1609(4)	6012(7)	48(4)
O(5)	5479(6)	2004(3)	5588(5)	71(3)
C(6)	5204(7)	443(4)	6213(6)	41(3)
O(6)	4504(5)	149(3)	5984(5)	64(3)
C(7)	7856(8)	1377(4)	6884(7)	50(4)
O(7)	8625(6)	1628(3)	7057(5)	82(3)
C(8)	7139(8)	762(4)	5337(7)	58(4)
O(8)	7526(6)	665(3)	4611(5)	80(3)
C(9)	6408(8)	2021(4)	8242(7)	54(4)
O(9)	7135(6)	2320(4)	8342(7)	105(4)
C(10)	3945(7)	1153(4)	7547(7)	45(3)
O(10)	3183(5)	940(3)	7213(5)	78(3)

[a] Equivalent isotropic *U* defined as one-third of the trace of the orthogonalized $\mathbf{U}_{ij}$ tensor.

Table 3. $C_{40}H_{37}IrO_{10}P_2Re_2$ (**4**): Selected Atomic Coordinates ($\times 10^4$) and Equivalent Isotropic Displacement Parameters (Å$^2 \times 10^3$)

	x	*y*	*z*	*U*(eq)[a]
Re(1)	4172(1)	9786(1)	1628(1)	34(1)
Re(2)	5092(1)	10134(1)	837(1)	32(1)
Ir(1)	5841(1)	8988(1)	1321(1)	33(1)
P(1)	3700(8)	10677(5)	1128(3)	39(6)
P(2)	7109(8)	8199(5)	1325(3)	41(6)
C(1)	3047(26)	9276(16)	1285(10)	36(9)
O(1)	2305(19)	9020(13)	1114(8)	60(7)
C(2)	5264(25)	10383(16)	1948(10)	36(9)
O(2)	5864(20)	10709(13)	2151(8)	67(8)
C(3)	3166(27)	10039(17)	1964(11)	50(11)
O(3)	2584(20)	10190(13)	2180(8)	69(8)
C(4)	4643(25)	9073(17)	2032(10)	38(9)
O(4)	4792(19)	8653(13)	2237(8)	64(8)
C(5)	6215(30)	9638(18)	656(12)	55(11)
O(5)	6926(17)	9444(11)	491(7)	45(7)
C(6)	6221(25)	10611(15)	1171(10)	28(8)
O(6)	7003(20)	10894(13)	1328(8)	71(8)
C(7)	5018(26)	10757(17)	419(11)	40(10)
O(7)	5009(20)	11158(13)	174(8)	71(8)
C(8)	3962(31)	9620(19)	476(12)	59(12)
O(8)	3287(19)	9320(12)	282(8)	56(7)
C(9)	6777(29)	9414(18)	1757(12)	52(11)
O(9)	7397(22)	9666(14)	2006(9)	83(10)
C(10)	4719(30)	8425(19)	1056(12)	54(11)
O(10)	4107(20)	8033(13)	946(8)	62(8)
Re(3)	2492(1)	4728(1)	1621(1)	32(1)
Re(4)	739(1)	5126(1)	848(1)	32(1)
Ir(2)	475(1)	3960(1)	1316(1)	34(1)
P(3)	2396(7)	5666(5)	1159(3)	34(6)
P(4)	−781(7)	3161(5)	1315(3)	33(6)
C(11)	1795(26)	5246(18)	1996(11)	47(10)
O(11)	1450(19)	5540(12)	2238(8)	62(8)
C(12)	3864(26)	4965(15)	1934(10)	38(9)
O(12)	4702(19)	5110(12)	2101(8)	64(8)
C(13)	2445(26)	4007(18)	2006(11)	44(10)
O(13)	2509(19)	3580(13)	2223(8)	65(8)
C(14)	3256(33)	4246(21)	1216(13)	70(14)
O(14)	3716(20)	3991(13)	1045(8)	60(8)
C(15)	1485(26)	4620(16)	477(11)	39(10)
O(15)	1932(20)	4329(13)	278(8)	67(8)
C(16)	363(27)	5763(18)	443(11)	45(10)
O(16)	169(19)	6167(13)	205(8)	64(8)
C(17)	−575(27)	4623(16)	660(10)	40(10)
O(17)	−1445(20)	4458(12)	490(8)	58(8)
C(18)	−64(31)	5606(20)	1171(13)	65(13)
O(18)	−477(21)	5919(14)	1415(9)	80(9)
C(19)	1261(27)	3434(17)	1023(11)	44(10)
O(19)	1806(18)	3035(12)	922(7)	52(7)
C(20)	−79(25)	4381(16)	1731(11)	38(9)
O(20)	−446(21)	4666(13)	1976(9)	76(9)

[a] Equivalent isotropic *U* defined as one-third of the trace of the orthogonalized $\mathbf{U}_{ij}$ tensor.

related triangulated compounds, as e.g. in $Re_2(\mu\text{-}PCy_2)(CO)_8(HgCl)$ where Δ(Re–Hg) is only 0.007 Å.[9] Therefore, these Re–M differences and the change of the exocyclic Re–M–P bond angles depend on electronic requirements. As is known, such structural distortions in **1** and **4** based on electronic requirements cannot be predicted by a symmetry change because they are determined by energetics.

The different bond lengths observed for two equivalent bonding sites of the dirhenium anions may be rationalized in terms of the lowered symmetry of the bipyramidal coordination sphere at the M atoms. Under C_1 symmetry in molecules of **1** and **4** the nonbonding orbital ($C_{2v}(d_{xy})$, a_2) occupied by an electron pair in the basis plane is lowered in energy. This leads to a stabilization of the bonding orbital to compensate the occupied antibonding orbital ($d_{x^2-y^2}$).[17,18] This stabilization exerts a trans influence leading to the structural differences along the Re–M edges. A strengthening of the Re(2)–M bond in **1** and **4** occurs in connection with a trans-positioned inert pair manifested through enlarged Re(1)–M–P bond angles. This is not observed in previously determined molecular structures of Rh(I) and Ir(I) complexes with a tbp ligand environment. The requirement of the chelating dirhenium anions of an acute bite angle in three-membered metal rings triggers this structural effect.

The bond lengths of M–C, M–P (M = Ir, Re, Rh), and Re–Re in **1** and **4** show, generally, no remarkable differences from those in related diorganophosphido-bridged dirhenium compounds described earlier.[19–21] Apart from the aforementioned deviations of the same M–Re bond lengths (M = Rh, Ir), the values of 2.943(1) and 3.034(1) Å in **1** and of average 2.912(2) and 3.012(2) Å in **4** are in the range of covalent single bond lengths, e.g. 2.914(1) Å in $Re(CO)_5Ir(CO)_3HRe(CO)_5$.[22] The shorter M–Re bond lengths are nearby or somewhat longer than supported Re–M (d^8–d^8) bond lengths in the following complexes: 2.970(1) Å in $RhRe(CO_3)(\mu\text{-}H)(\mu\text{-}SEt)(dppm)_2$ (dppm = bis(diphenylphosphino)methane),[23] 2.851(1) Å in $[RhReCH_3(CO)_4(dppm)_2][CF_3SO_3]\cdot 3CH_2Cl_2$,[16] and 2.914(3) and 2.830(3) Å in $Re_2Ir(\mu\text{-}PPh_2)[\mu\text{-}OC(CH_2)_3CH_3](CO)_8PPh_3$.[24] This structural feature is reminiscent of analogous bridged homometallic metal–metal bonds in complexes. Further known heterobimetallics contain Re–M(d^4–d^8) twofold bridged bond lengths of 2.936(1) Å in $[(PCy_2)_2ReH)(\mu\text{-}PCy_2)_2Rh\cdot 1.5COD]BF_4$ and of 2.912(1) Å in $(PCy_2)(CO)_2Re(\mu\text{-}PCy_2)_2Ir(CO)_2PCy_2$,[25] which are also close to the shorter Re–M bond lengths in **1** and **4**. Finally, for the metal–metal lengths in the considered Re_2M rings, it might be striking on the basis of M atom single bond covalent radii that both homo- and heterometallic bond lengths are shortened by the exchange of the smaller Rh vs the bigger homologeous Ir atom,

---

(17) Albright, T. A.; Burdett, J. K.; Whangbo, M.-H. *Orbital Interaction in Chemistry*; Wiley: New York, 1985.

(18) Albright, T. A.; Kang, S.-K.; Arif, A. M.; Bard, A. J.; Jones, R. J.; Leland, J. K.; Schwab, S. T. *Inorg. Chem.* **1988**, *27*, 1246.

(19) Haupt, H.-J.; Flörke, U.; Schnieder, H. *Acta Crystallogr.* **1991**, *C47*, 2304.

(20) LaPlaca, S. J.; Ibers, J. A. *Acta Crystallogr.* **1965**, *18*, 511.

(21) Payne, C. N.; Ibers, J. A. *Inorg. Chem.* **1969**, *8*, 2714.

(22) Breimair, J.; Robl, C.; Beck, W. *J. Organomet. Chem.* **1991**, *411*, 395.

(23) Antonelli, D. M.; Cowie, M. *Inorg. Chem.* **1990**, *9*, 1818.

(24) Flörke, U.; Schirmer, W.; Haupt, H.-J. Unpublished results.

(25) Baker, T. R.; Calabrese, J. C.; Glassmann, T. E. *Organometallics* **1988**, *7*, 1889.

Table 4. $C_{56}H_{52}O_8P_3Re_2Rh\cdot CHCl_3$ (**6**): Selected Atomic Coordinates ($\times 10^4$) and Equivalent Isotropic Displacement Parameters ($Å^2 \times 10^3$)

	x	*y*	*z*	*U*(eq)[a]
Re(1)	7201(1)	1275(1)	7586(1)	35(1)
Re(2)	9746(1)	1175(1)	7694(1)	34(1)
Rh(1)	8340(1)	1399(1)	6073(1)	31(1)
P(1)	6436(2)	689(1)	8426(2)	38(1)
P(2)	7729(2)	1602(1)	4563(2)	34(1)
P(3)	10138(2)	1370(1)	6068(2)	35(1)
C(1)	5788(8)	1447(3)	7331(7)	53(2)
O(1)	4933(6)	1555(3)	7154(6)	80(1)
C(2)	7299(8)	1608(3)	8754(7)	51(2)
O(2)	7446(7)	1818(2)	9408(6)	84(1)
C(3)	7504(7)	879(3)	6465(6)	30(1)
O(3)	7511(5)	574(2)	6025(4)	45(1)
C(4)	7660(8)	1815(3)	6947(7)	47(2)
O(4)	7710(6)	2177(2)	6885(5)	61(1)
C(5)	9248(8)	1005(3)	8933(7)	45(1)
O(5)	9060(6)	924(2)	9702(5)	56(1)
C(6)	11205(8)	1123(3)	8108(7)	51(2)
O(6)	12083(6)	1071(3)	8332(6)	78(1)
C(7)	9715(8)	1752(3)	8203(7)	54(2)
O(7)	9714(7)	2070(2)	8559(5)	73(1)
C(8)	9682(7)	589(3)	7223(7)	44(1)
O(8)	9683(6)	259(2)	6948(6)	63(1)

[a] Equivalent isotropic *U* defined as one-third of the trace of the orthogonalized U_{ij} tensor.

Table 5. Selected Bond Lengths (Å) and Angles (deg)

$C_{40}H_{25}O_{10}P_2Re_2Rh$ (**1**)			
Bond Lengths			
Re(1)–Re(2)	3.169(1)	Re(1)–Rh(1)	3.034(1)
Re(2)–Rh(1)	2.943(1)	Re(1)–P(1)	2.438(2)
Re(2)–P(1)	2.416(2)	Rh(1)–P(2)	2.315(2)
Bond Angles			
Re(1)–Re(2)–Rh(1)	59.4(1)	Re(1)–Rh(1)–Re(2)	64.0(1)
Re(1)–Re(2)–P(1)	49.6(1)	Re(2)–Rh(10–P(2)	137.9(1)
Rh(1)–Re(2)–P(1)	108.9(1)	Re(1)–Rh(1)–P(2)	158.1(1)
Re(2)–Re(1)–Rh(1)	56.6(1)	C(9)–Rh(1)–C(10)	167.0(4)
Re(2)–Re(1)–P(1)	49.0(1)	Re(1)–P(1)–Re(2)	81.5(1)
Rh(1)–Re(1)–P(1)	105.5(1)		
$C_{40}H_{37}IrO_{10}P_2Re_2$ (**4**)			
Bond Lengths			
Re(1)–Re(2)	3.124(2)	Re(3)–Re(4)	3.143(2)
Re(1)–Ir(1)	3.007(2)	Re(3)–Ir(2)	3.017(2)
Re(1)–P(1)	2.465(10)	Re(3)–P(3)	2.452(9)
Re(2)–Ir(1)	2.912(2)	Re(4)–Ir(2)	2.912(2)
Re(2)–P(1)	2.437(9)	Re(4)–P(3)	2.427(8)
Ir(1)–P(2)	2.291(9)	Ir(2)–P(4)	2.296(9)
Bond Angles			
Re(2)–Re(1)–Ir(1)	56.7(1)	P(2)–Rh(1)–P(3)	106.4(1)
Re(2)–Re(1)–P(1)	50.0(2)	P(2)–Rh(1)–C(3)	109.0(2)
Ir(1)–Re(1)–P(1)	106.6(2)	P(2)–Rh(1)–C(4)	103.6(3)
Re(1)–Re(2)–Ir(1)	59.6(1)	P(3)–Rh(1)–C(3)	120.1(2)
Re(1)–Re(2)–P(1)	50.8(2)	P(3)–Rh(1)–C(4)	119.6(3)
P(1)–Re(1)–C(1)	84.8(3)	C(3)–Rh(1)–C(4)	96.9(4)
P(1)–Re(1)–C(2)	91.3(3)	Re(2)–P(3)–Rh(1)	74.8(1)
C(1)–Re(1)–C(2)	90.1(4)	Re(1)–C(3)–Rh(1)	80.5(3)
P(1)–Re(1)–C(3)	89.7(2)	Re(1)–C(3)–O(3)	158.2(7)
P(1)–Re(1)–C94)	171.6(3)	Rh(1)–C(3)–O(3)	121.2(6)
C(3)–Re(1)–C(4)	96.5(4)	Re(1)–C(4)–Rh(1)	81.7(4)
Re(1)–Re(2)–Rh(1)	51.3(1)	Re(1)–C(4)–O(4)	153.0(8)
Rh(1)–Re(2)–P(3)	50.2(1)	Rh(1)–C(4)–O(4)	125.3(7)
P(3)–Re(2)–C(6)	92.6(3)	Ir(1)–Re(2)–P(1)	110.4(2)
P(3)–Re(2)–C(7)	96.0(3)	Re(1)–Ir(1)–Re(2)	63.7(1)
P(3)–Re(2)–C(8)	86.6(3)	Re(1)–Ir(1)–P(2)	158.3(2)
C(5)–Re(2)–C(6)	94.4(4)	Re(2)–Ir(1)–P(2)	137.7(2)
C(5)–Re(2)–C(7)	85.8(4)	C(9)–Ir(1)–C(10)	158.7(15)
C(5)–Re(2)–C(8)	91.3(4)	Re(1)–P(1)–Re(2)	79.2(3)
C(6)–Re(2)–C(7)	91.0(4)	Re(4)–Re(3)–Ir(2)	56.4(1)
C(6)–Re(2)–C(8)	92.0(4)	Re(4)–Re(3)–P(3)	49.5(2)
Re(1)–Rh(1)–Re(2)	71.5(1)	Ir(2)–Re(3)–P(3)	105.9(2)
Re(1)–Rh(1)–P(2)	127.0(1)	Re(3)–Re(4)–Ir(2)	59.6(1)
Re(1)–Rh(1)–P(3)	126.4(1)	Re(3)–Re(4)–P(3)	50.3(2)
Re(1)–Rh(1)–C(3)	49.8(2)	Ir(2)–Re(4)–P(3)	109.9(2)
Re(1)–Rh(1)–C(4)	49.3(3)	Re(3)–Ir(2)–Re(4)	64.0(1)
Re(2)–Rh(1)–P(2)	161.4(1)	Re(3)–Ir(2)–P(4)	157.6(2)
Re(2)–Rh(1)–P(3)	55.0(1)	Re(4)–Ir(2)–P(4)	138.2(2)
Re(2)–Rh(1)–C(3)	83.9(2)	C(19)–Ir(2)–C(20)	164.6(14)
Re(2)–Rh(1)–C(4)	87.6(3)	Re(3)–P(3)–Re(4)	80.2(3)
$C_{56}H_{52}O_8P_3Re_2Rh\cdot CHCl_3$ (**6**)			
Bond Lengths			
Re(1)–Re(2)	3.255(1)	Rh(1)–P(2)	2.295(2)
Re(1)–Rh(1)	2.681(1)	Rh(1)–P(3)	2.297(2)
Re(1)–P(1)	2.457(3)	Rh(1)–C(3)	2.073(8)
Re(1)–C(3)	2.076(8)	Rh(1)–C(4)	2.046(9)
Re(1)–C(4)	2.055(10)	C(3)–O(3)	1.160(10)
Re(2)–Rh(1)	2.883(1)	C(4)–O(4)	1.168(12)
Re(2)–P(3)	2.447(2)		
Bond Angles			
Re(2)–Re(1)–Rh(1)	57.1(1)	Rh(1)–Re(1)–P(1)	138.4(1)
Re(2)–Re(1)–P(1)	109.3(1)	Rh(1)–Re(1)–C(3)	49.7(2)
Re(2)–Re(1)–C(3)	74.7(2)	Rh(1)–Re(1)–C(4)	49.0(3)
Re(2)–Re(1)–C(4)	77.9(3)		

although the reciprocal behavior should be expected. The origin of this effect depends on the replacement of diphenyl (–M effect) vs dicyclohexyl (+I effect) groups at the bridging phosphorous atom which cause a shortening of Re–Re bonds, as is known from the complexes $Re_2(\mu\text{-}PR_2)(\mu\text{-}H)(CO)_8$ (R = Ph, Cy).[26]

On the basis of known MO descriptions of dihydrophosphido-bridged triangular clusters such alterations of metal–metal bond lengths reflect the extent of mixing symmetry-adapted bridging nonmetal orbitals and metal–metal orbitals in the region of frontier orbitals.[17,18]

Cluster Complex 6. The unifold unsaturated triangular title compound with C_1 symmetry has a Re_2Rh ring as a central fragment of which one Re(1)–Rh edge is bridged by two carbonyls, the other is bridged by a dicyclohexylphosphido group, and the Re–Re edge remains unbridged. The coordination of the metal atoms is completed by the subsequent terminal ligands: the Re(1) atom has three ligands (2 CO, PPh_3), the Re(2) four carbonyls, and the Rh one PPh_3. Each Re atom reaches with the bridging and terminal ligand atoms an octahedrally distorted ligand environment (Figure 3).

The rhodium atom [4 + 2]-coordination pattern of four nonmetal and two metal atoms fulfills the demand of six as cn but has no striking relationship with an coordination octahedron. For example, if P(2) and the Re(2) atom, reasonably, are selected as comprising the apex in this polyhedron, the bond angles subtended at the Rh with the four nonmetal ligand atoms give an average value of 109.3°. If the differences between the nonmetal atom bond angles subtended at Rh (see Table 5) are neglected, the given average value corresponds with a pseudotetrahedral shaped nonmetal ligand atom environment. Such ligand geometry might be advantageous to develop metal–metal π bonding interaction effects.[27]

The structural bonding pattern between the Re(1) and Rh atoms displays an electronic deficit which is more effective at Rh than at Re(1) and inclines the C–O bond vector in the direction of the Rh atom. This behavior is similar to that of semibridging carbonyls and best described as the initial state in a trajectory of a CO migration process.[28] Furthermore, the tendency of this fragment to realize a butterfly like geometry with a dihedral angle of 19.8° between the best planes of $ReRh(\mu\text{-}CO)_2$ instead of a planar geometry might also depend on the mentioned imbalance of the electronic unsaturation. However, such an effect is not strong enough to be reflected by significant differences of the endocyclic bond angles and bond lengths in $Re(1)Rh(\mu\text{-}CO)_2$: Re–C(3)–Rh = 80.5(3)°, Re–C(4)–Rh = 81.7(4)°, Re–C(3) = 2.076(8) Å, Rh–C(3) = 2.073(8) Å, Re–C(4) = 2.055(10)

---

(26) Flörke, U.; Haupt, H.-J. *Z. Krist.* **1992**, *201*, 295.

(27) Barr, R. D.; Green, M.; Howard, J.; Marder, T. B.; Orpen, G. A.; Stone, F. G. A. *J. Chem. Soc., Dalton Trans.* **1984**, 2757.

(28) Crabtree, R. H.; Lavin, M. *Inorg. Chem.* **1986**, *25*, 805.

Å, Rh–C(4) = 2.046(9) Å. They are even close to those of the symmetrically bridged carbonyls in the homometallic planar fragment $Rh_2(\mu\text{-}CO)_2$ in $MoRh_2(\mu\text{-}CO)_2(CO)_5(\eta\text{-}C_5Me_5)_2$(Rh═Rh): average Rh–C–Rh = 82.2(1)° and average Rh–C = 1.999(3) Å. For the last-named compound with a central Rh_2-Mo metal ring a MO description was developed on the basis of C_{2v} symmetry.[27] The Re_2Rh metal ring in **6** has three different ring angles of 71.5(1)° at Rh, of 57.1(1)° at Re(1), and of 51.3(1)° at Re(2). This correlates with a reduction of opposite metal–metal bond lengths of 3.255(1) Å (Re–Re), 2.883(1) Å (Rh–Re(2)), and 2.681(1) Å (Rh–Re(1)) as expected. The shorter of both Rh–Re bond lengths is a π bond which is necessary to fulfill the demand of the noble gas rule. To our knowledge such a π(Re–Rh) bond length was determined for the first time.

Fenske has noted that the dominant bonding interaction in related homometallic complexes with a double bond bridged by two carbonyls occurs through the bridging ligands rather than through direct interaction between transition metal atoms.[29] It is, therefore, not unreasonable that a similar interaction pattern which is additionally modified by different acceptor abilities of the metal atoms also applies to the covalent Re–Rh bond doubly bridged by two carbonyls in **6**. In contrast the second Re–Rh bond has single bond character compared to the unbridged bond of 2.943(1) Å in **1**. Finally, the unsupported Re–Re bond length of 3.255(1) Å being strongly elongated with respect to that of 3.104(1) Å in $Re_2(CO)_{10}$ has to be considered.[30] This bond is necessary to avoid two opposite vacant coordination sites, which are untypical for the dirhenium ring members. It should be a weak metal–metal contact being more sensitive than the supported heterometallic bonds for electronic requirements of a Re_2Rh ring. In terms of the isolobal concept, the cluster **6** can be regarded as an inorganic cyclopropene ring with the tendency of opening its unsupported Re–Re edge to form perhaps a biradical system. From the structural viewpoint, samples like **5** and **6** might be rare.

Supplementary Material Available: Lists of complete atomic coordinates, bond distances and angles, anisotropic displacement parameters, and hydrogen atom coordinates for compounds **1**, **4**, and **6** (20 pages). Ordering information is given on any current masthead page.

---

(29) Schugart, K. A.; Fenske, R. F. *J. Am. Chem. Soc.* **1979**, *108*, 5094.

(30) Churchill, M. R.; Amoh, K. N.; Wassermann, H. J. *Inorg. Chem.* **1981**, *20*, 1609.